Evans

CALIFORNIA INSTITUTE OF TECHNOLOGY

ANTENNA LABORATORY

Technical Report No. 81

HIGHER-ORDER DFB LASERS WITH MULTIPLE PERIODICITIES

by
Dwight L. Jaggard
and
Gary A. Evans

September 1976

SECTION 1. INTRODUCTION

There has been continued interest in distributed feedback (DFB) lasers since the pioneering work of Kogelnik and Shank [1,2] in 1971-72. Their work described the threshold characteristics of transversely unbounded periodic media at the first Bragg order or resonance (i.e., the case $N = 1$ in Bragg's Law $\lambda = 2\Lambda/N$ where λ is the wavelength of the propagating wave and Λ is the fundamental spatial period of the structure). Since then there has been much additional work at the first Bragg order [3-5], including the case of transversely bounded DFB lasers [6]. In 1972 Bjorkholm and Shank [7] experimentally demonstrated the first higher-order DFB laser (i.e., $N \geq 2$) with output at the second and third Bragg resonances. Recently there has been additional experimental work at the second Bragg order [8] and interest in multiply-resonant DFB lasers [9].

It is the purpose of this paper to use the extended coupled waves (ECW) theory [10] to find explicit values for the coupling coefficient and the phase mismatch at the first three Bragg resonances for several periodicity profiles. These results are displayed in the form of dispersion diagrams. The expressions for coupling and phase mismatch can then be used in the threshold expressions of Kogelnik and Shank [1]. Explicit results are found for the threshold gain, the mode spectra and the critical length for oscillation of the lowest-order longitudinal mode at all Bragg resonances for both index and gain coupling. Several plots are given to show how threshold gain varies with Bragg order N for singly-periodic media and how the threshold gain varies for different multiply-periodic structures at the second Bragg order. The cases of sinusoidal,

$$\left.\begin{aligned} F_1'(z) - i\delta_N F_1(z) &= i\chi_N^{+} B_1(z) \\ -B_1'(z) - i\delta_N B_1(z) &= i\chi_N^{-} F_1(z) \end{aligned}\right\} \tag{3}$$

where $\chi_N^{\pm} = \begin{cases} \chi_N & \text{for cosinusoidal perturbations} \\ \pm i\chi_N & \text{for sinusoidal perturbations} \end{cases}$

and where the primes denote differentiation with respect to the longitudinal coordinate z. The coupling coefficient χ_N is a measure of the field exchange per unit length between the waves $F_1(z)$ and $B_1(z)$. The phase mismatch δ_N represents the phase shift per unit length from the resonance condition where maximum coupling occurs. Explicitly, the values of δ_N and χ_N can be found for singly-periodic media [10].

$$\chi_N = (-1)^{N+1} \frac{k^2 \varepsilon_r \eta^N}{2^{N+1} \beta_o} \frac{1}{\Pi^* g_n} \tag{4}$$

$$\delta_N = \frac{k^2 \varepsilon \{1 - \zeta_N (n/2)^2 [\frac{N^2}{2(N^2-1)}]\} - \beta_o^2}{2\beta_o} \tag{5}$$

where $\zeta_N = \begin{cases} 0 & \text{for } N = 1 \\ 1 & \text{otherwise} \end{cases}$

$$g_n = \{4n(n-N)/N^2\}^2$$

$$\Pi^* g_n = \begin{cases} \prod_{n=1}^{(N-1)/2} g_n & \text{for N odd} \\ \prod_{n=1}^{N/2} g_n & \text{for N even} \\ 1 & \text{for N = 1} \end{cases}$$

$$\beta_o = NK/2 = k_o \varepsilon_r^{1/2}$$

$$\Delta\beta_N = \beta - \beta_o$$

$$\Delta k_N = k - k_o$$

At the first Bragg resonance, the above equations reduce to well-known results [1,11]. The bandgap shift is the value of $\Delta k_N \varepsilon^{1/2}/K$ where $\delta_N/K = 0$. From Equation (4) it can be shown that this value is proportional to η^2. Note that the coupling is proportional to η^N.

For the periodicity profiles under consideration, the Fourier components f_p are

$$\text{square-wave} \qquad f_p = \begin{cases} 1/p & p \text{ odd} \\ 0 & p \text{ even} \end{cases} \tag{6}$$

$$\text{triangular-wave} \qquad f_p = \begin{cases} \dfrac{(-1)^{(p-1)/2}}{p^2} & p \text{ odd} \\ 0 & p \text{ even} \end{cases} \tag{7}$$

$$\text{sawtooth} \qquad f_p = \frac{(-1)^{(p+1)}}{p} \qquad p \text{ odd,even} \tag{8}$$

where the appropriate cosine or sine series is used in the expression for the dielectric constant (1) and where $f_1 \equiv 1$ is the normalization for all profiles.

At the first Bragg resonance, the ηf_1 term makes the major contribution to both the coupling and the phase mismatch for all periodicity profiles. Hence, δ_1 and χ_1 are identical to the usual value found for singly-periodic media in (4) and (5). The expressions for δ_N and χ_N are

shown in Tables 1 and 2 for the cases N = 1,2,3. The explicit calculations are given in Reference 12 and follow the method of calculation demonstrated in Reference 10. Two things should be noted. First, the phase mismatch is mostly dependent upon the largest Fourier component, hence the bandgap shift depends upon $(\eta f_1)^2$ and is approximately equal for all the periodicity profiles considered at a given Bragg order. Second, the major contribution to the coupling coefficient at the N^{th} Bragg resonance is due to the term ηf_N if $\eta f_N \neq 0$. Therefore, the value of χ_N is significantly smaller when f_N does not exist (e.g., with sinusoidal, square- and triangular-wave profiles when N = 2) than when it does exist (e.g., sawtooth profile when N = 2). To exemplify the results of the above calculations, the dispersion diagram which relates the free-space wave number k to the longitudinal wave number β is plotted in Figure 1. The dispersion relation is

$$\Delta\beta_N^2 = \delta_N^2 - \chi_N^2 \tag{9}$$

for waves that propagate as $e^{i\beta z} = e^{i(\beta_o + \Delta\beta_N)z}$. Figure 1 displays the effects of four different periodicity profiles on the dispersion diagram at the second Bragg resonance for the case $\eta f_1 = 0.05$. The normalized coupling χ_2/K is equivalent to the maximum value of $\mathrm{Im}\{\Delta\beta_2/K\}$. The sawtooth profile, which has a finite Fourier component f_2, has a larger coupling coefficient than do the other examples which have coupling coefficients $O(\eta f_1)$ smaller. For typical values of perturbation, such as $\eta f_1 \sim 10^{-2}$-10^{-5}, the differences would be greatly magnified. All bandgaps are approximately centered at the same frequency since the phase mismatch for all four profiles is similar. In the dispersion diagrams

	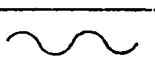	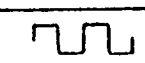	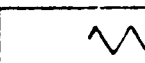	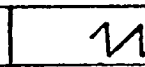
N = 1	$\frac{\Delta k \epsilon^{\frac{1}{2}}}{K}$	$\frac{\Delta k \epsilon^{\frac{1}{2}}}{K}$	$\frac{\Delta k \epsilon^{\frac{1}{2}}}{K}$	$\frac{\Delta k \epsilon^{\frac{1}{2}}}{K}$
N = 2	$\frac{\Delta k \epsilon^{\frac{1}{2}}}{K} - \frac{\eta^2}{12}$	$\frac{\Delta k \epsilon^{\frac{1}{2}}}{K} - \frac{\eta^2}{12}(0.91)$	$\frac{\Delta k \epsilon^{\frac{1}{2}}}{K} - \frac{\eta^2}{12}(0.99)$	$\frac{\Delta k \epsilon^{\frac{1}{2}}}{K} - \frac{\eta^2}{12}(0.95)$
N = 3	$\frac{\Delta k \epsilon^{\frac{1}{2}}}{K} - \frac{27\eta^2}{256}$	$\frac{\Delta k \epsilon^{\frac{1}{2}}}{K} - \frac{27\eta^2}{256}$	$\frac{\Delta k \epsilon^{\frac{1}{2}}}{K} - \frac{27\eta^2}{256}$	$\frac{\Delta k \epsilon^{\frac{1}{2}}}{K} - \frac{\eta^2}{12}$

Table 1 - Normalized phase mismatch δ_N/K for several periodicity profiles at the first three Bragg orders

	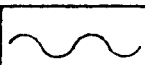		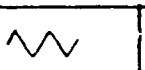	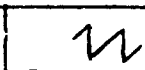
N = 1	$\frac{\eta}{8}$	$\frac{\eta}{8}$	$\frac{\eta}{8}$	$\frac{\eta}{8}$
N = 2	$\frac{-\eta^2}{8}$	$\frac{-\eta^2}{8}(0.77)$	$\frac{-\eta^2}{8}(0.93)$	$\frac{\eta}{8}$
N = 3	$\frac{243\,\eta^3}{2048}$	$\frac{\eta}{8}$	$\frac{\eta}{24}$	$\frac{\eta}{8}$

Table 2 - Normalized coupling coefficient χ_N/K for several periodicity profiles at the first three Bragg orders.

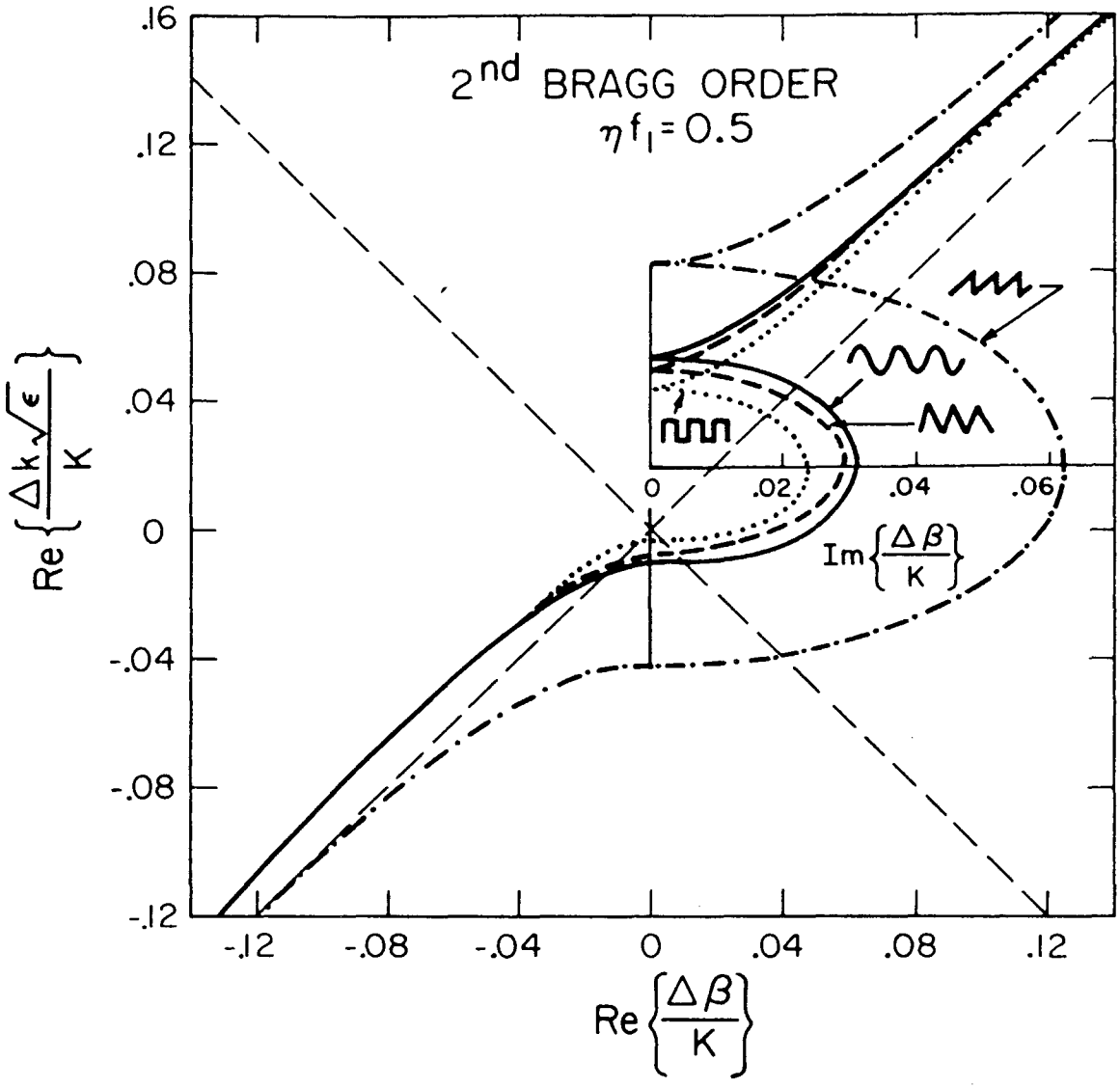

Figure 1. Dispersion diagram at the second Bragg order for several periodicity profiles. The strength of the fundamental Fourier component is $\eta f_1 = 0.5$ for each profile. Only the sawtooth profile has a Fourier component ηf_2 which causes the relatively large band-gap and coupling. The imaginary values of the longitudinal wave number are given by the elliptical portions of the plot and the separate scale. The medium is lossless ($\epsilon_i/\epsilon_r = 0$).

the bandgap shift is demonstrated by the fact that the center of the bandgap is not located at the value $\Delta k\varepsilon^{1/2}/K = 0$. Note that upward bandgap shifts occur for index coupling (i.e., $\eta^2 > 0$) and downward bandgap shifts occur for gain coupling (i.e., $\eta^2 < 0$). We note that at the third Bragg order and at all other odd orders (not shown) the dispersion diagram would contain similar curves for the square-wave, triangular-wave and sawtooth profiles. However, the sinusoidal profile produces coupling coefficients and bandgap sizes that are $O(\eta f_1)^{N-1}$ smaller. Hence, the curve for the sinusoidal profile would differ considerably from the other three curves. That is, the bandgap and the coupling coefficient would be relatively small. Similar results occur if the gain is modulated. However, in this case the bandgaps would be inverted (i.e., have imaginary values of $\Delta k\varepsilon^{1/2}/K$) at all odd Bragg orders. This can be seen from expressions (4), (5) and (9). Gain modulation at even Bragg orders produces dispersion diagrams that are similar to the index modulation case except for the previously mentioned change in the sign of the bandgap shift. The nature of the occurrence of inverting or non-inverting bandgaps is a result of the sign of the term η^N in Equation (4) for χ_N/K. This in turn depends upon the oddness or evenness of N and the type of coupling (i.e., $\eta = \eta_r$ or $\eta = i\eta_i$).

SECTION 3. DFB THRESHOLD GAIN AND MODE SPECTRA

The previous values for the phase mismatch and the coupling coefficient can be used directly in the results of Kogelnik and Shank [1] for DFB threshold gain and longitudinal mode spectra. One condition must be fulfilled, however. The dominant coupling must come from the

periodicity and not from the boundaries in order that the ECW equations remain valid [12]. Therefore, the periodic media must be many cycles in length. Explicitly this condition is given as

$$K\ell >> (2/n)^{N-1} \tag{10}$$

where ℓ is the length of the structure. In practical cases, the above length restriction can be relaxed if the periodicity amplitude is tapered at the ends of the structure. This reduces the boundary coupling. A similar boundary effect has been noted in quantum mechanical scattering [13].

Following the work of Kogelnik and Shank, we find the exact threshold condition when the boundary conditions are applied to the ECW equations

$$\frac{D_N - i\delta_N}{D_N + i\delta_N} e^{2D_N\ell} = -1 \tag{11}$$

where $D_N = (\chi_N^2 - \delta_N^2)^{1/2}$. We define the quantities Δ_N and G_N by the equation

$$\delta_N \equiv \Delta_N - iG_N$$

where Δ_N is proportional to the bandgap shift and G_N is proportional to the gain. Note the approximate equality

$$G_N\ell \simeq -k\epsilon_r^{1/2}\ell[\epsilon_i/(2\epsilon_r)]$$

which holds for small perturbations and singly periodic media. The high- and low-gain approximations hold when $|n/2|^N << |\epsilon_i/\epsilon_r|$ or $|n/2|^N >> |\epsilon_i/\epsilon_r|$, respectively, for the first few Bragg orders.

The high-gain case gives a threshold gain approximation of

$$4(G_N^2 + \Delta_N^2) = \chi_N \chi_N^* e^{2G_N \ell} \tag{12}$$

for the normalized gain G_N (where the asterisk denotes complex conjugate) and a longitudinal mode spectrum

$$\tan^{-1}(\Delta_N/G_N) - \Delta_N \ell = (m + 1/2)\pi + \text{phase}(\chi_N)$$
$$(m = 0, \pm 1, \pm 2, \cdots) \tag{13}$$

for the normalized frequency Δ_N. Figure 2 shows a sketch of the higher Bragg order ($N \geq 2$) mode spectrum for the first few longitudinal modes for the case of index coupling ($\eta = \eta_r$) and the case of gain coupling ($\eta = i\eta_i$). For index coupling (Figure 2a), the gain symmetrically pushes the modes out from the usual two mirror cavity case (shown by the dashed lines). However, the bandgap shift produces an asymmetry with respect to exact Bragg resonance and shifts the entire spectrum toward higher frequencies. Figure 2b,c shows the spectrum for gain coupling at odd and even Bragg orders, respectively. For odd Bragg orders, oscillation is possible near Bragg resonance, but the bandgap shift prevents oscillation exactly at Bragg resonance $\Delta k \varepsilon_r^{1/2}/K = 0$. Even-order gain coupling is similar to even-order index coupling except for the sign of the bandgap shift. Hence, the mode spectrum for higher Bragg orders is not symmetric. This is different from the symmetric first-order case [1]. This asymmetry is not surprising since the bandgap shift is positive for index coupling and negative for gain coupling whenever $N \geq 2$. One should note that a small asymmetry occurs even in the first-order case. However,

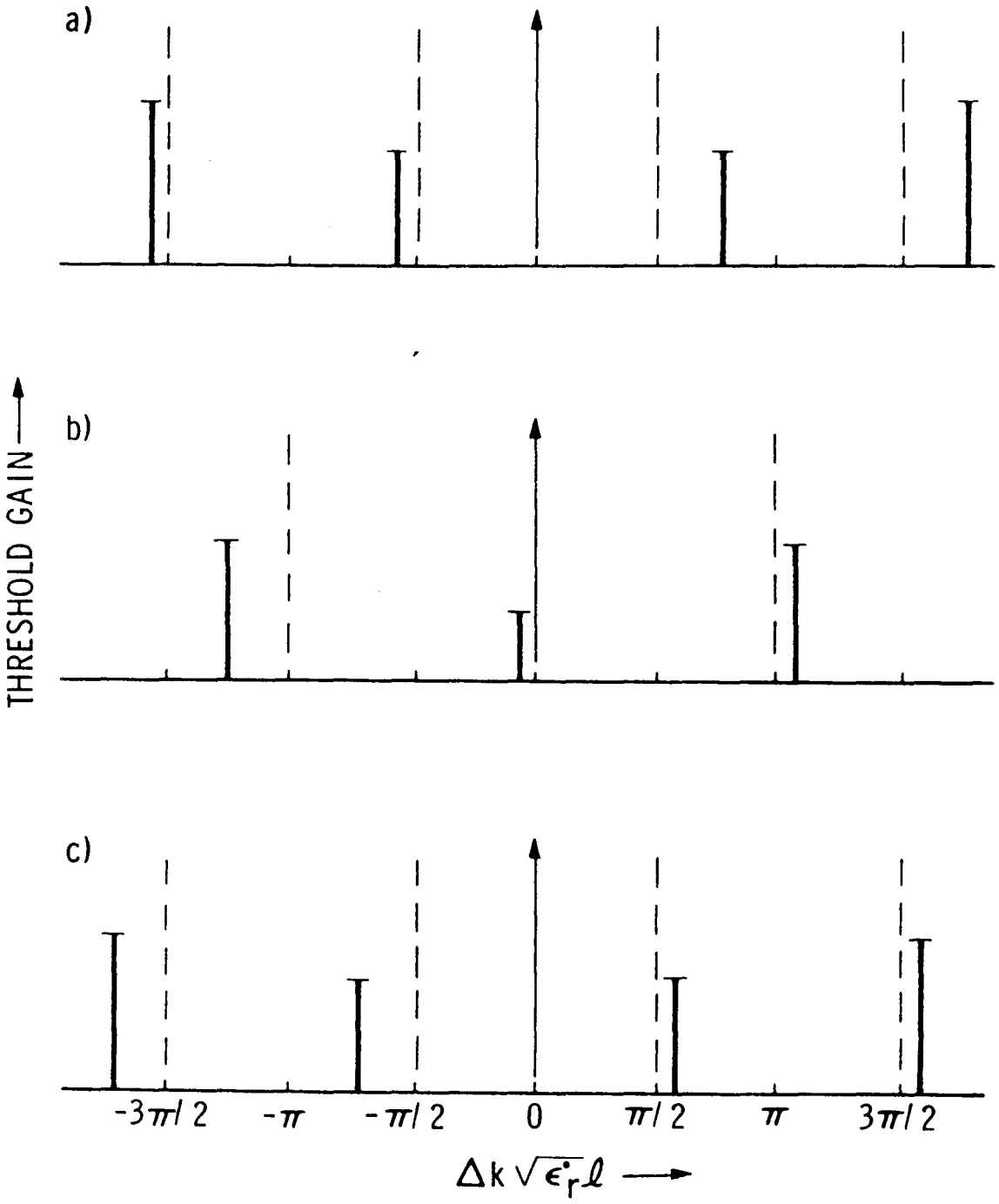

Figure 2. Sketch of the mode spectrum from higher-order DFB lasers for: (a) index coupling (N=2,3,4,···); (b) gain coupling (N=3,5,7,···); (c) gain coupling (N=2,4,6,···) in the high-gain regime. Note the asymmetries produced by the bandgap shift.

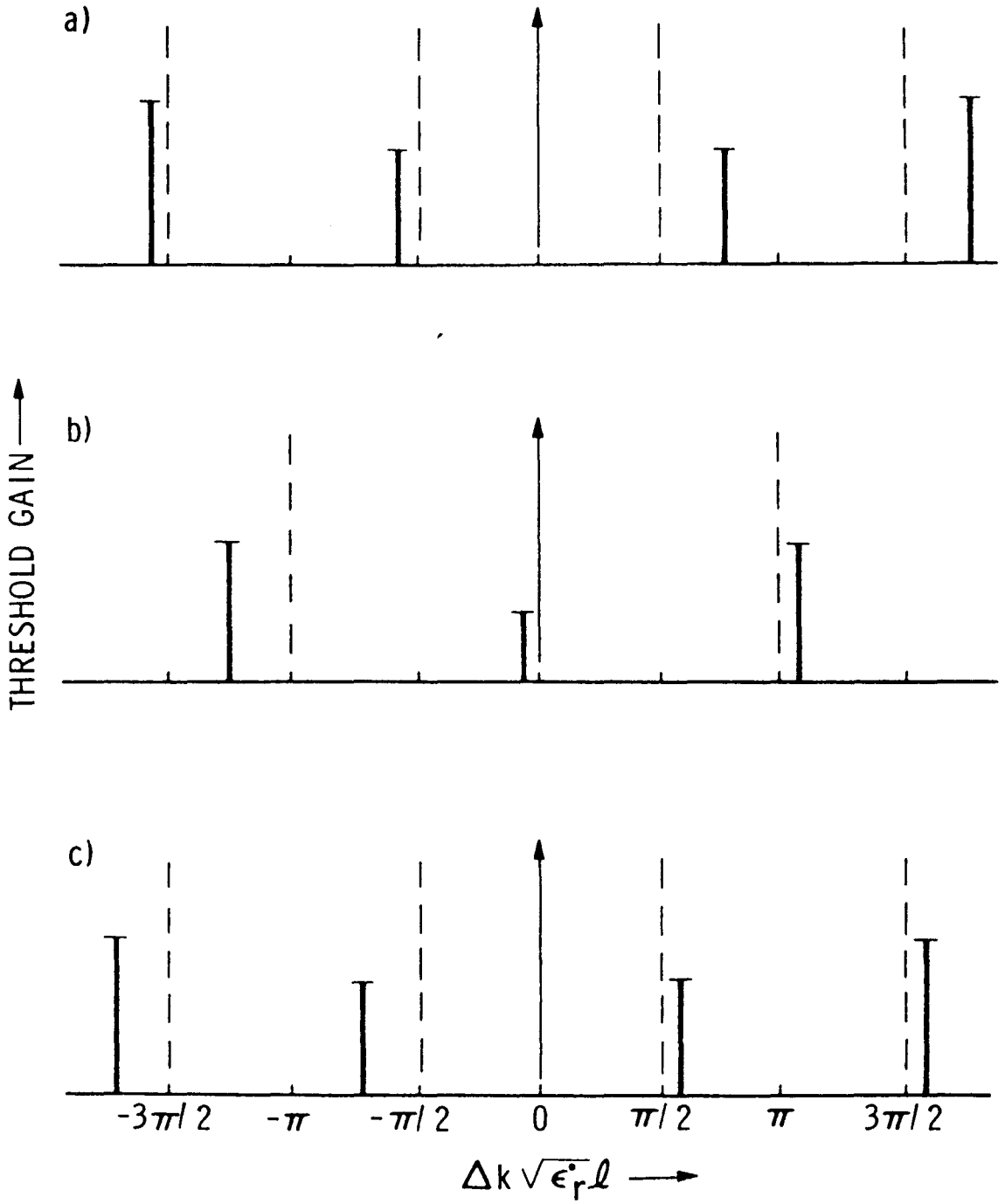

Figure 2. Sketch of the mode spectrum from higher-order DFB lasers for: (a) index coupling (N=2,3,4,···); (b) gain coupling (N=3,5,7,···); (c) gain coupling (N=2,4,6,···) in the high-gain regime. Note the asymmetries produced by the bandgap shift.

the finite bandgap shift which causes the asymmetry is found from the exact Floquet analysis and not from the coupled waves analysis [12].

In the low-gain approximation, only the lowest-order longitudinal mode characteristics are given. For index coupling, the lowest-order (m=1) longitudinal mode frequency or wave number is given by

$$\Delta_N^2 - \chi_N^2 = 6/\ell^2 \xrightarrow[K\ell\to\infty]{} 0 \tag{14}$$

Thus, oscillation occurs at the bandgap edges given by $\Delta_N = \pm\chi_N$ for long structures. The threshold gain for this longitudinal mode is given by

$$G_N\ell \simeq \frac{3}{\Delta_N\chi_N\ell^2} \xrightarrow{K\ell\to\infty} \frac{3}{(\chi_N\ell)^2} \tag{15}$$

This relation can be alternatively written as

$$\varepsilon_i/\varepsilon_r \simeq -192[(\pi/2)^{2N}\,(NK\ell)^3]^{-1} \tag{16}$$

for singly periodic media at the first few Bragg resonances. It can be shown that this result also holds for even-order gain coupling. Note that positive average gain (i.e., $\varepsilon_i/\varepsilon_r < 0$ or $G_N\ell > 0$) is needed for oscillation.

In the low-gain approximation for odd-order gain coupling, the oscillation of the lowest-order (m=0) longitudinal mode takes place at the bandgap center

$$\Delta_N = 0 \tag{17}$$

with the threshold gain condition

$$\chi_N^2 + G_N^2 = -6/(|\chi_N|\ell^3) \xrightarrow[K\ell\to\infty]{} 0 \tag{18}$$

This can be further approximated for singly periodic media by

$$\varepsilon_i/\varepsilon_r \simeq |\eta/2|^N \tag{19}$$

for long structures operating at the first few Bragg resonances. Since the threshold gain is negative for odd-order gain coupling (i.e., $\varepsilon_i/\varepsilon_r > 0$ or $G_N\ell < 0$), one can find the critical length ℓ_c which is necessary for the start of oscillation from the condition $G_N = 0$. This quantity is given by

$$|\chi_N|\ \ell_c = 3^{1/2} \tag{20}$$

and is similar to previous results for the first-order case [1]. Oscillation occurs whenever the structure length ℓ satisfies the condition $\ell \geq \ell_c$.

In Figure 3 the threshold gain of the lowest-order longitudinal mode is shown as a function of normalized length. The plots are shown for the case of index coupling at the first four Bragg orders when $\eta_r f_1 = 10^{-2}$. Note that for $0 < \eta_r k \varepsilon_r^{1/2} \ell/4 < 5$, all the curves are in the high-gain region for $N \geq 2$. Although the coupling varies as η^N from Equation (4), the threshold gain only varies approximately as $N\eta$ in the high-gain region. Hence, the operation of higher-order DFB lasers requires only a gain increase $O(N)$ over the first-order case. However, the high-gain region implies "under-coupling" with the result that the spatial distribution of intensity has large maxima at the ends of the periodic structure [1]. If it is desirable to operate in the region

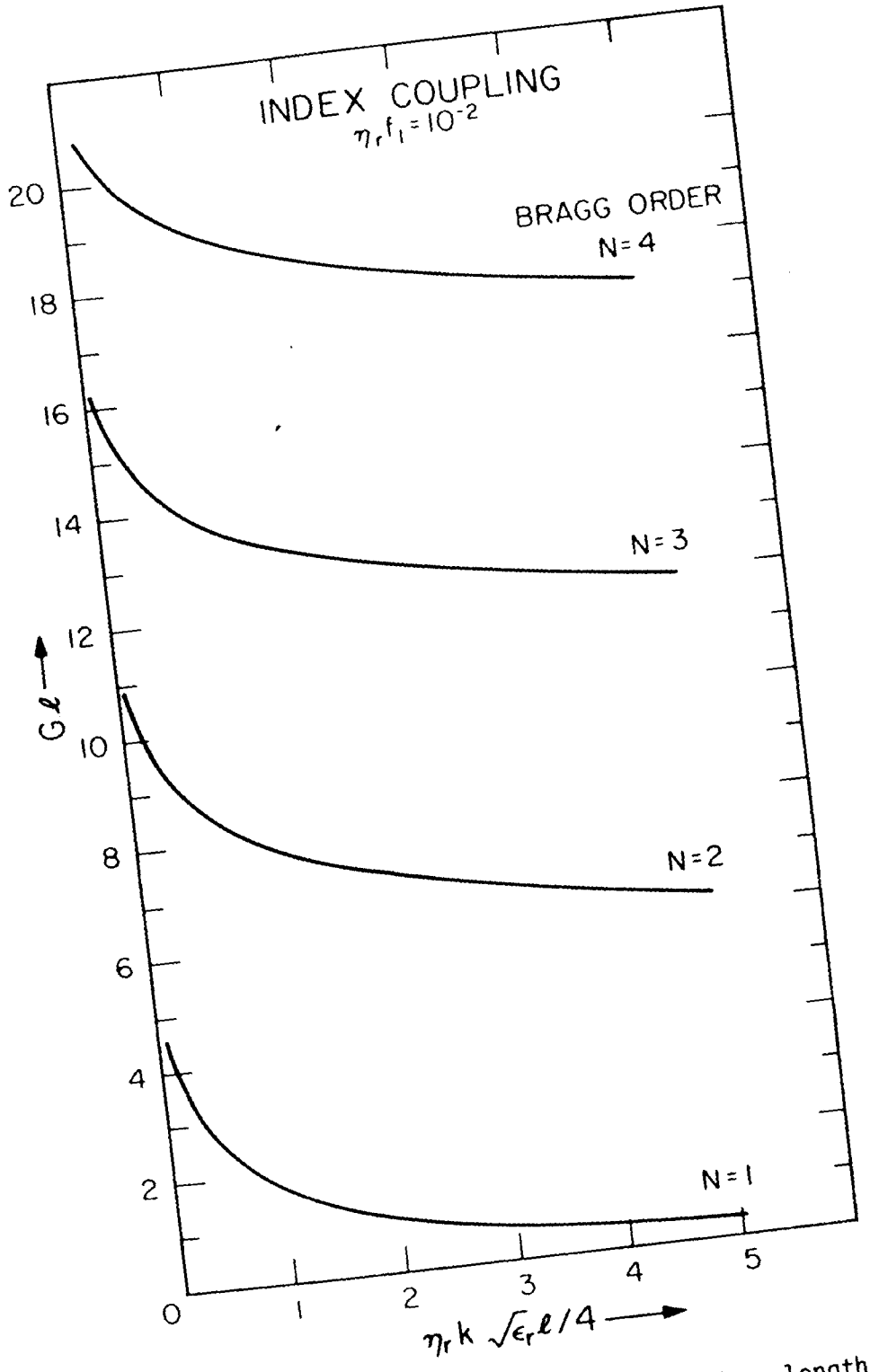

Figure 3. Threshold gain as a function of normalized length and Bragg order for singly-periodic media with index coupling and $\eta f_1 = 10^{-2}$. The curves are in the high-gain regime for $N \geq 2$ since $G\ell > 5$.

$\chi_N \ell \simeq 1$ so that a more uniform intensity distribution occurs, it is necessary to increase the normalized length $K\ell$ by a factor $(\eta/2)^{1-N}$ over that of the first order case. This may be difficult unless the perturbation is realtively large. The low-gain regime which typically occurs for $G\ell \lesssim 0.5$ (not shown for $N \geq 2$) demonstrates a different behavior from the high-gain case. As shown by (16), the threshold gain is proportional to $(\eta/2)^{2N}$ in the low-gain case. Thus, the gain requirements are increased by a factor of $(\eta/2)^2$ with each increase in Bragg order for singly-periodic media. Although the threshold gain is small, it varies significantly with Bragg order unlike the high-gain case.

The threshold characteristics for gain coupling are identical to the index coupling characteristics at even Bragg orders and, in the high-gain approximation, at odd Bragg orders. Figure 4 shows the variation of the threshold gain as a function of normalized length. Plots are given at the first four Bragg orders for singly-periodic gain coupled media when $\eta_i f_1 = 10^{-2}$. As before, only the lowest-order longitudinal mode characteristics are shown. As expected, for odd Bragg orders, the threshold gain becomes zero at the value $\ell = \ell_C$ and negative for larger lengths. Thus, in the region close to zero threshold gain, the threshold gain curves for odd and even orders intersect near the values of ℓ_C given by (20). This is shown in Figure 4 near the value $\eta_i k \epsilon_r^{1/2} \ell/4 \simeq 5 \times 10^4$ for the cases N = 2,3. The fact that the average gain is negative does not mean that no gain is present in the structure. The oscillation or threshold gain condition is only satisfied when there are portions of the structure with gain. Zero threshold gain

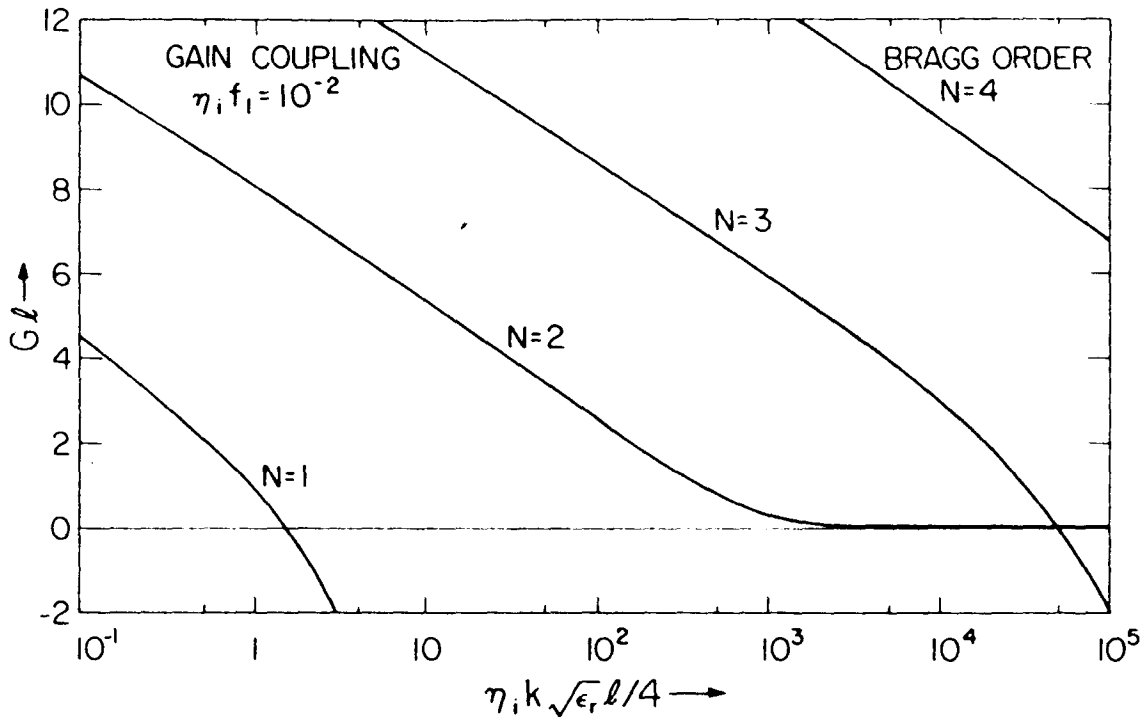

Figure 4. Threshold gain as a function of normalized length and Bragg order for singly-periodic media with gain coupling and $\eta f_1 = i10^{-2}$. For odd Bragg orders negative threshold gain is possible.

implies that the structure alternately has regions of gain and loss. It occurs when $\ell = \ell_C$.

It is interesting to note that these results concerning threshold gain values in the low-gain approximation are identical to the results of the infinite medium case where stability criteria determine the threshold characteristics [14]. It should also be noted that in the case of even-order coupling, the threshold gain can be reduced by using a combination of both index and gain coupling in the low-gain regime. The threshold gain that results from using both coupling types is smaller than the value that would be obtained by using a single type of coupling [12]. However, in the case of odd-order coupling, the threshold gain cannot be reduced below the value obtained by gain coupling. The mixed coupling case results (not shown) can be derived from an appropriate expansion of Equation (11).

As a final example, consider the threshold gain characteristics for several periodicity profiles as shown in Figure 5. We consider the case of index coupling and $nf_1 = 10^{-2}$ at the second Bragg order. The sawtooth wave has a Fourier component f_2 and hence has threshold characteristics that are similar to the first order case shown in Figure 3. However, the sinusoidal, trangular-wave and square-wave profiles have only odd-order Fourier components, and hence the threshold gain characteristics are similar to the second Bragg order threshold gain of Figure 3. Figure 5 is typical of all even Bragg order threshold gains for these profiles. All odd Bragg order threshold gains will be somewhat similar to the N = 1 curve of Figure 3. As noted previously, large differences

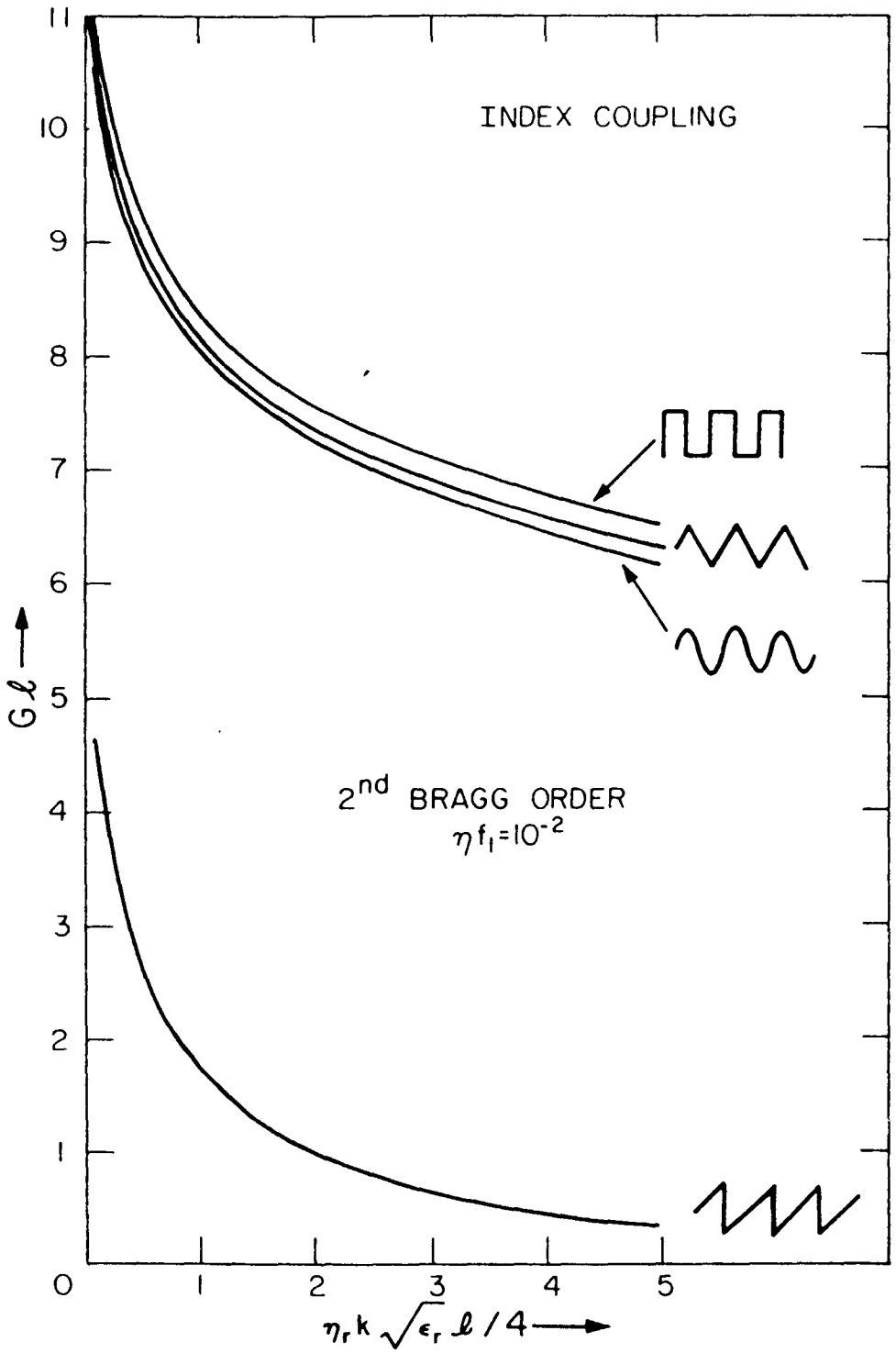

Figure 5. Threshold gain as a function of normalized length and periodicity profile at the second Bragg order with index coupling and $\eta f_1 = 10^{-2}$. Note the lowered threshold of the sawtooth profile due to a finite Fourier component ηf_2. (Compare to Figure 1).

in the coupling cause only small differences in the threshold gain in the high-gain regime. These differences in threshold gain become more pronounced in the low-gain regime. The beginning of this effect can be seen at the value $\eta_r k\epsilon_r^{1/2}\ell/4 \simeq 5$. Since index and gain coupling characteristics are identical in the high-gain regime, Figure 5 represents gain coupling characteristics as well as index characteristics for $G\ell \geq 5$.

SECTION 4. DISCUSSION AND CONCLUSIONS

The previous sections extended the first-order results of Kogelnik and Shank [1] to higher Bragg orders. Values for the coupling and phase mismatch have been given in Tables 1 and 2 for typical periodicity profiles. The results of the analysis for DFB lasers are given below. We particularly note the reduction in threshold gain which occurs through the use of multiply-periodic structures and the use of both index and gain coupling.

1. In the high-gain approximation, the mode spectrum is asymmetrically shifted from exact Bragg resonance to higher (for index coupling) or lower (for gain coupling) frequencies when $N \geq 2$.

2. In the low-gain approximation, oscillation takes place at the bandgap edges (for index and even-order gain coupling) or at the bandgap center (for odd-order gain coupling).

3. Although bandgap size and coupling coefficients vary as η^N, the threshold gain only varies roughly as $N\eta$ in the high-gain approximation for singly periodic media. In the low gain region, the threshold gain varies as $|\eta|^{-2N}$ for index coupling and even-order gain coupling or as $|\eta|^N$ for odd-order gain coupling.

4. Threshold gains for gain coupling are similar to the index coupled case except in the low-gain approximation for odd Bragg orders. In this case, the threshold gain can become negative. The critical length for oscillation with zero threshold gain is given by $\ell_C = 3^{1/2}/(\chi_N)$. For even Bragg orders, the positive threshold gain can be reduced by using a combination of both index and gain coupling.

5. Threshold gains can be reduced significantly at the N^{th} Bragg order if the periodicity profile has a Fourier component $f_N \neq 0$. The reduction becomes more significant for smaller threshold gains.

The calculations in this paper are based on a transversely unbounded mediumwith non-saturating gain. Calculations involving bounded media with radiation losses and involving nonlinear effects are saved for future work.

ACKNOWLEDGMENTS

We acknowledge the helpful discussions with Dr. C. Elachi (JPL) and Professor C. H. Papas (Caltech).

REFERENCES

1. H. Kogelnik and C. Shank, "Coupled Wave Theory of Distributed Feedback Lasers," J. Appl. Phys., Vol. 43, pp. 2327-2335, 1972.
2. H. Kogelnik and C. Shank, "Stimulated Emission in a Periodic Structure," Appl. Phys. Lett., Vol. 18, pp. 152-154, 1971.
3. S. Wang, "Principles of Distributed Feedback and Distributed Bragg-Reflector Lasers," IEEE JQE, Vol. QE-10, pp. 413-425, 1974.
4. S. Chinn, "Effects of Mirror Reflectivity in a Distributed-Feedback Laser," IEEE JQE, Vol. QE-9, pp. 574-580, 1973.
5. R. Shubert, "Theory of Optical Waveguide Distributed Lasers with Non-uniform Gain and Coupling," J. Appl. Phys., Vol. 45, pp. 209-215, 1974.
6. C. Elachi, G. Evans, and C. Yeh, "Transversely Bounded DFB Lasers," J. Opt. Soc. Am., Vol. 65, pp. 404-412, 1975.
7. J. Bjorkholm and C. Shank, "Higher-Order Distributed Feedback Oscillators," Appl. Phys. Lett., Vol. 20, pp. 306-308, 1972.
8. Z. Alferov, S. Gurevich, V. Kuchinsky, M. Mizerov, E. Portnoy, and M. Reich, "Investigation of GaAs/GaAlAs Waveguide Lasers with Second Order Distributed Feedback," Proceedings of Integrated Optics Conference, Salt Lake City, Utah, January 12-14, 1976.
9. H. Stoll and D. Seib, "Multiply Resonant Distributed-Feedback Lasers," IEEE JQE, Vol. QE-12, pp. 53-57, 1976.

10. D. Jaggard and C. Elachi, "Floquet and Coupled-Waves Analysis of Higher-Order Bragg Coupling in a Periodic Medium," J. Opt. Soc. Am., Vol. 66, pp. 674-682, 1976.

11. H. Kogelnik, "Coupled Wave Theory for Thick Hologram Gratings," Bell Sys. Tech. J., Vol. 48, pp. 2909-2947, 1969.

12. D. Jaggard, "Bragg Interactions in Periodic Media," Caltech Ant. Lab. Report No. 75, August 1976.

13. R. Feynman and A. Hibbs, Quantum Mechanics and Path Integrals, New York, McGraw-Hill, 1965.

14. D. Jaggard, "Stability of Higher Order Bragg Interactions in Active Periodic Media," submitted for publication.